Analysis of Non-Tidal Loading Deformation at VLBI Sites

S. Singh, J. Böhm, H. Krásná, N. Balasubramanian, O. Dikshit

Abstract Very Long Baseline Interferometry (VLBI) is one of the geodetic techniques used to establish the International Terrestrial Reference Frame (ITRF). It relies on data collected from multiple antennas situated at various locations across the Earth's surface. However, the accuracy of VLBI measurements can be compromised by Earth's crust deformation caused by a range of geophysical factors, including plate tectonics, solid Earth tide-induced loading, atmospheric pressure variations, and redistribution of water masses, both over land and in the oceans. Among these factors, non-tidal loading (NTL) deformations can also lead to positional shifts in VLBI sites, thus affecting measurement accuracy. To address these NTL effects in VLBI analysis, geophysical models are employed to correct the displacement of VLBI stations. The objective of this study is to compare the NTL products obtained from different loading services, such as the VieAPL, ESMGFZ, IMLS, and EOST. The evaluation of how these NTL products impact VLBI analysis is carried out using the VieVS software. This assessment entails the computation of baseline length repeatability and station height standard deviation, both before and after applying the loading corrections.

Keywords Non-tidal loading, VLBI, VieVS

Shivangi Singh · Nagarajan Balasubramanian · Onkar Dikshit
Geoinformatics, Department of Civil Engineering, IIT Kanpur, Kanpur, Uttar Pradesh 208016, India

Johannes Böhm · Hana Krásná
Department of Geodesy and Geoinformation, TU Wien, Wiedner Hauptstraße 8-10, 1040 Vienna, Austria

1 Introduction

The establishment and maintenance of the ITRF and International Terrestrial Reference System (ITRS) represent essential endeavours in modern geodesy. These efforts are pivotal because they provide the foundation for measuring and interpreting geophysical phenomena and their impact on Earth's shape and orientation. Geophysical factors, such as post-glacial rebound, seismic events, and variations in Earth's rotation, induce deformations in the Earth's surface. Consequently, accurate correction models are required to maintain the stability and accuracy of the reference frame, as they can introduce significant discrepancies in geodetic measurements (Altamimi et al., 2016). Calculating the displacements due to various geophysical effects allows us to reduce them from the station coordinates, obtaining the long-term linear station motion. Unlike other geophysical models, NTL models are not accurate enough. Therefore, it is advised not to adjust station positions for these effects, as per the International Earth Rotation and Reference Systems Service (IERS) Convention 2010. In recent years, numerous studies have been conducted on specific space geodetic techniques aimed at reducing non-tidal loading effects (Schuh et al., 2004; Petrov and Boy , 2004; Eriksson and MacMillan , 2014; Roggenbuck et al., 2015; Glomsda et al., 2020).
Non-tidal loading effects displace geodetic stations by a few centimetres on an annual to sub-daily basis (Wijaya et al., 2013). Also, the Global Geodetic Observing System (GGOS) was established with the ambitious objective of achieving 1mm accuracy in determining Earth's geometric parameters, as outlined in its strategic plan. Pursuing such unprecedented accuracy has revitalized the focus on correcting NTL effects, given

their substantial impact on geodetic measurements and the realization of GGOS's objectives.

2 NTL components and loading services

In this section, we will elucidate the NTL components employed in our investigation, the sources from which this data is extracted and the process of standardizing data from various services to ensure uniform formatting for comparison. In geodesy, NTL data refers to the utilization of diverse geophysical models aimed at correcting the theoretical signal delay encountered during VLBI observations. These models encompass non-tidal atmospheric loading (NTAL), non-tidal oceanic loading (NTOL), and hydrological loading (HYDL), which can be employed either independently or in combination to address the cumulative loading effects. NTAL is specifically designed to consider the impact of atmospheric pressure fluctuations on the Earth's surface, arising from dynamic changes in atmospheric pressure driven by meteorological events and factors unrelated to tidal forces. HYDL, on the other hand, addresses the deformation of the Earth's crust resulting from shifts in continental water storage. Lastly, NTOL is concerned with the deformation of the Earth's crust caused by the redistribution of mass within the oceans.

The displacement data resulting from these three loading factors is obtained from four distinct sources, which are as follows:
1. VieAPL (Vienna Atmospheric Pressure Loading) (https://vmf.geo.tuwien.ac.at/products.html)
2. ESMGFZ (Earth-System-Modelling group at GFZ)(http://rz-vm115.gfz-potsdam.de:8080/repository)
3. IMLS (International Mass Loading Service)(http://massloading.net/)
4. EOST (École & observatoire des sciences de la Terre)(http://loading.u-strasbg.fr/index.php)

VieAPL, IMLS, and EOST provide users with both pre-calculated global Grid-based mass loading time series and pre-calculated time series customized for particular space geodesy stations. Furthermore, IMLS enhances its offerings by delivering an on-demand Internet service, granting users the capability to request data for specific stations and specify their desired time intervals. In parallel, ESMGFZ delivers pre-computed global Grid-based mass loading time series and also allows users the option to retrieve data for particular stations while tailoring the time ranges according to their requirements. Within each loading category, numerous models are available for generating the associated loading products. In our study, the choice of models for different loading categories and services depends on factors such as data availability, time steps, update frequency, and spatial resolution level. Table 1 presents the characteristics of the chosen models. VieAPL and ESMGFZ data is updated daily, while IMLS data is updated monthly. EOST data undergoes updates every few months.

After selecting models for each loading category and service, we acquired center-of-mass frame NTL data for the year 2020 for this study. We identified a total of 163 VLBI stations, which remained consistent across all services and were categorized as ITRF sites. Following the data extraction process, the next pivotal step involves data formatting. It's important to note that data obtained from different services come in various formats. To facilitate meaningful comparisons within VieVS, we formatted the data obtained from the models selected from EOST, IMLS, and ESMGFZ into the VieAPL format of the loading corrections.

3 Data comparison

To compare the NTL products from four different services, we initiate the process by generating a time series graph illustrating NTAL displacement. This initial step is crucial because VieAPL exclusively offers NTAL data. It's worth highlighting that the NTAL products derived from all four services display a substantial level of concurrence among them (see Figure 1). This alignment can be ascribed to the fact that all services utilize the ECMWF model for extracting loading data.

In addition to the NTAL displacement graph, we generate another time series graph to evaluate the cumulative sum of all NTL components. It is evident that most services demonstrate a high degree of agreement among themselves in the cumulative NTL trend (see Figure 2). However, it's worth highlighting that there is a significant deviation observed, particu-

Table 1 Attributes of the selected non-tidal loading models corresponding to different loading components of various services.

Service	Loading	Model	Spatial Resolution	Time-steps	Data Availability
VieAPL	NTAL	ECMWF	1° × 1°	6h	1994-present
IMLS	NTAL	MERRA2	2' × 2'	6h	1980-present
IMLS	NTOL	MPIOM06	2' × 2'	3h	1980-present
IMLS	HYDL	MERRA2	2' × 2'	3h	1980-present
EOST	NTAL	ECMWF	0.5° × 0.5°	3h	2000-present
EOST	NTOL	ECCO1	1° × 1°	12h	1993-2021
EOST	HYDL	GLDAS2	0.25° × 0.25°	3h	2000-2022
ESMGFZ	NTAL	ECMWF	0.5° × 0.5°	3h	1976-present
ESMGFZ	NTOL	MPIOM	1° × 1°	3h	1976-present
ESMGFZ	HYDL	LSDM	0.5° × 0.5°	24h	1976-present

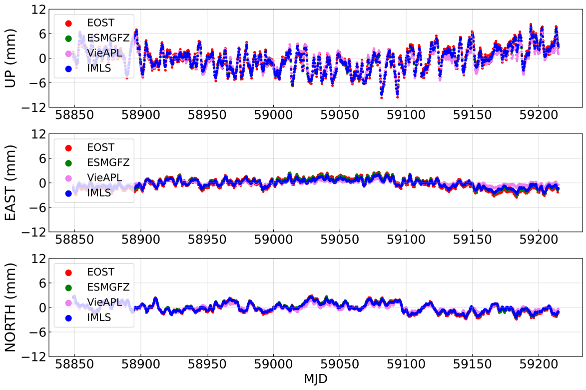

Fig. 1 Site displacement time series due to NTAL in CM-frame at AGGO station.

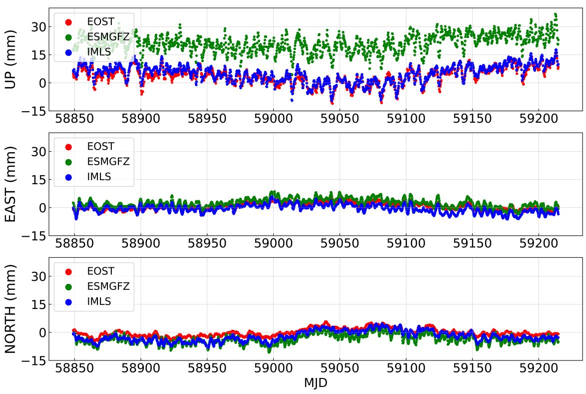

Fig. 2 Site displacement time series due to all NTL components in CM-frame at AGGO station.

larly in the up component of ESMGFZ.

To gain insight into the variations in data related to each NTL component of different services, we've plotted Root Mean Square (RMS) values of the difference in site displacement due to NTL between two services in the CM-frame and for 163 VLBI stations (refer to Figures 3,4,5). The RMS values are organized based on the latitude of each respective VLBI station. Notably, we observe significant RMS values of more than 8 mm, mainly occurring within the latitude range of 30°N to 65°N, particularly in the Up direction. Among the different loading components, the NTAL component shows the least variation between the two services, while the HYDL component exhibits the most substantial differences. This discrepancy is especially pronounced in the case of HYDL component of ESMGFZ vs. EOST, with an average RMS value of 6.7 mm and a maximum RMS value of 18.5 mm for the up direction. These disparities can be attributed to the use of distinct models with varying resolutions by different services. Additionally, the separate treatment of Sea Level Loading (SLEL) in order to achieve global mass conservation, as undertaken by ESMGFZ, may contribute to this observed variation. In contrast, other services incorporate partial mass conservation in both NTOL and HYDL, which could influence the level of agreement in these components.

4 Data processing in VieVS

We investigated the influence of non-tidal loading displacement models within VLBI analysis. These displacements resulting from non-tidal loading were incorporated as adjustments to the station coordinates at the observation level. The entire processing was conducted using VieVS, utilizing a one-year process list of R1/R4 sessions and OPT files for the year 2020. Notably, the VieVS graphical user interface (GUI) initially featured the option for loading displacement due to NTAL data, and subsequently, options for NTOL

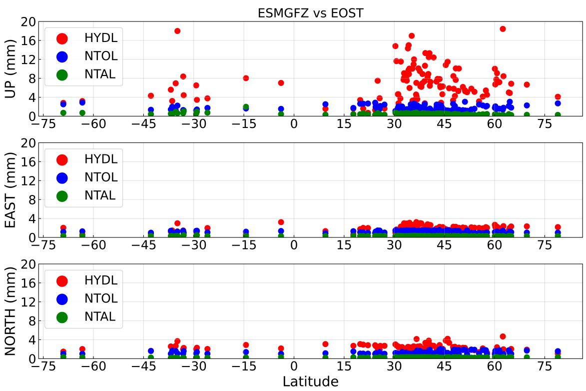

Fig. 3 RMS values of difference of site displacement due to different NTL components between ESMGFZ and EOST in CM-frame. The RMS values of stations are organized latitude-wise.

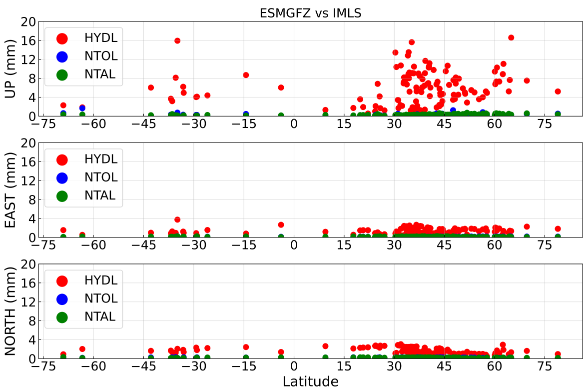

Fig. 4 RMS values of difference of site displacement due to different NTL components between ESMGFZ and IMLS in CM-frame. The RMS values of stations are organized latitude-wise.

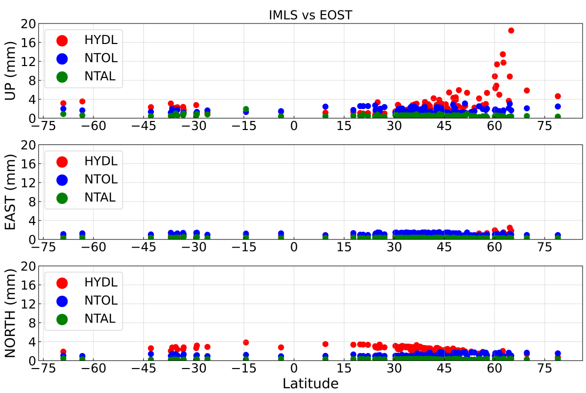

Fig. 5 RMS values of difference of site displacement due to different NTL components between IMLS and EOST in CM-frame. The RMS values of stations are organized latitude-wise.

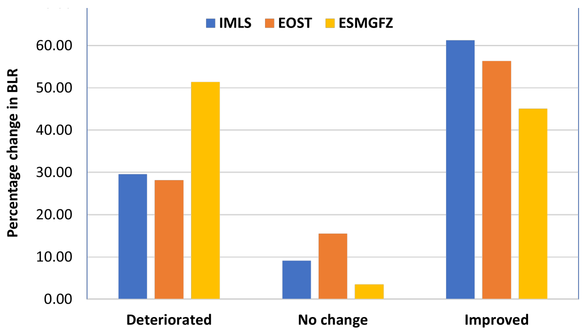

Fig. 6 Percentage change in BLR before and after applying all NTL models in CM-frame for 142 baseline.

and HYDL were introduced later in the process.

In VLBI analysis, the term "baseline length repeatability" (BLR) denotes the degree of precision in measuring the length of a baseline connecting two VLBI stations over a period of time. BLR holds significant importance in VLBI because it directly influences the accuracy of both geodetic and astrometric measurements. By assessing BLR before and after applying NTL displacement products, we can determine whether there is an improvement in BLR as a result of using NTL models. In Figure 6, we present the percentage change in BLR before and after incorporating all NTL data, focusing on a total of 29 stations. The results reveal that 71.83% of baselines demonstrate improvement or remain unchanged when using EOST data, while 70.4% of baselines show improvement or stability with IMLS data. In contrast, only 48.59% of baselines exhibit improvement or stability when utilizing ESMGFZ data. Likewise, we've computed the standard deviation of station heights both before and after the application of NTL models for a total of 142 baselines (see Figure 7). The result revealed that a total of 67% of station height standard deviation improves after the application of NTL in the case of EOST and IMLS. However, in the case of ESMGFZ, the improvement is only 52.38%.

5 Conclusions and outlook

The application of NTL displacement corrections to VLBI station coordinates is essential for achieving high-precision BLR. It helps reduce systematic errors,

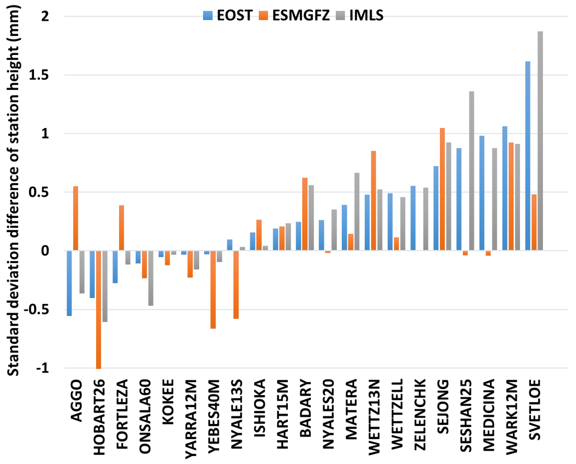

Fig. 7 Difference in the standard deviation of station heights both before and after the application of NTL models in CM-frame for 21 stations.

improve station coordinate accuracy, and enhance the long-term stability of VLBI measurements. Variation in the improvement of BLR among services (see Figure 6) is primarily due to HYDL and NTOL. The standard deviation difference of the time series of station height with and without NTL shows that the estimation of station coordinates improves upon the application of NTL models (see Figure 7). Also, results from different services are consistent with each other except in the case of ESMGFZ. The distinct approach taken by ESMGFZ in addressing Sea Level Loading (SLEL) with a focus on global mass conservation might be a contributing factor to the observed variation. In order to enhance our understanding, we will incorporate a broader range of data spanning approximately 20 years. We expect that this extended timeframe will provide valuable insights and contribute to a more comprehensive analysis.

Acknowledgement

This research has received joint support from the Austrian Agency for International Cooperation in Education and Research (OeAD-GmbH) and the National Centre for Geodesy (NCG), India.

References

Altamimi Z, Rebischung P, Métivier L, & Collilieux X (2016) ITRF2014: A new release of the International Terrestrial Reference Frame modeling nonlinear station motions. *Journal of Geophysical Research: Solid Earth*, 121(8), 6109-6131, doi: 10.1002/2016JB013098.

Böhm J, Böhm S, Boisits J, Girdiuk A, Gruber J, Hellerschmied A, Krásná H, Landskron D, Madzak M, Mayer D, McCallum J, McCallum L, Schartner M, Teke K (2018) Vienna VLBI and Satellite Software (VieVS) for Geodesy and Astrometry. *Publications of the Astronomical Society of the Pacific*, doi: 10.1088/1538-3873/AAA22B.

Dill, R., & Dobslaw, H. (2013) Numerical simulations of global-scale high-resolution hydrological crustal deformations. *Journal of Geophysical Research: Solid Earth*, 118, doi: 10.1002/jgrb.50353.

Eriksson D, MacMillan DS (2014) Continental hydrology loading observed by VLBI measurements. *Journal of Geodesy*, 88:675–690, doi: 10.1007/s00190-014-0713-0.

Glomsda M, Bloßfeld M, Seitz M, Seitz F (2020) Benefits of non-tidal loading applied at distinct levels in VLBI analysis. *Journal of Geodesy*, doi: 10.1007/s00190-020-01418-z.

Petrov L, Boy J P (2004) Study of the atmospheric pressure loading signal in very long baseline interferometry observations. *Journal of Geophysical Research*, 109(B3):B03405, doi: 10.1029/2003JB002500.

Roggenbuck O, Thaller D, Engelhardt G, Franke S, Dach R, Steigenberger P (2015) Loading-induced deformation due to atmosphere, ocean and hydrology: model comparisons and the impact on global SLR, VLBI and GNSS Solutions. *T. van Dam (eds), REFAG 2014, International Association of Geodesy Symposia, Vol. 146, Springer International Publishing Switzerland*, pp. 71-77, doi: ISBN:978-3-319-45628-7.

Schuh H, Estermann G, Crétaux J F, Bergé-Nguyen M, & van Dam T (2004) Investigation of hydrological and atmospheric loading by space geodetic techniques. *In Satellite Altimetry for Geodesy, Geophysics and Oceanography: Proceedings of the International Workshop on Satellite Altimetry, a joint workshop of IAG Section III Special Study Group SSG3. 186 and IAG Section II, September 8–13, 2002, Wuhan, China. Springer Berlin Heidelberg*, pp. 123-132, doi: 10.1007/978-3-642-18861-9_15.

Wijaya DD, Böhm J, Karbon M, Krásná H, & Schuh H (2013) Atmospheric pressure loading. *In: Böhm J, Schuh H (eds) Atmospheric effects in space geodesy. Springer, Berlin, Heidelberg*, pp 137–157, doi: 10.1007/978-3-642-36932-2_4.